



MINESWEEPER STUDENT PROJECT FALL 2007

REPORT ON THE DEVELOPMENT OF STEERING SYSTEM FOR MINESWEEPER

Advisor:

Professor Ephrahim Garcia

Compiled by:

**Yong Sheng Khoo
Franklin Geeng
Greg Meess**

Content Page

1. SUMMARY

2. INTRODUCTION

2.1 Objectives and Needs

2.2 Design Choices

3. DETAILED DISCUSSIONS

3.1 Calculations of Steering Torque

3.2 Gear Reduction Calculations

3.3 Stress Analysis on Various Components

3.4 Encoder

3.5 Prototyping

4. CONCLUSIONS

Steering Specifications

Parts List and Cost

Future Plan

5. APPENDIX A (Matlab Code)

6. APPENDIX B (Drawings)

1. SUMMARY

The report presents the design of the steering system for Gladiator – the IGVC competition robot. The design utilizes motors, gears, pulleys, belts and encoders to generate the desired steering configurations. Spur gears are utilized to generate the opposing turning direction, belts and pulleys are used to transmit the torque produced by the motor to steer the wheels. Absolute magnetic encoders are used to control the desired turning angle of the wheels. In this design, the overall objectives were met. Our steering system is able to make the desired direction – going straight, turning left and right, and zero-point-turn. This design gives us advantages for the IGVC competition.

2. INTRODUCTION

The steering sub team has to provide a design to steer the vehicle at the IGVC competition during summer 2008. Before starting any design, we started out surveying of the competition ground. During summer 2007, a group of five people were sent to the IGVC competition site at Oakland University, Michigan. Having gone to the site, the team has a better understanding of the obstacle course event of the competition. The competition course was laid out in a big field with artificial incline of 15%, sand pit with depth of 2-3 inches, and obstacles placed randomly. The obstacles on the site consist of construction drums, cones, pedestals and barricades. All the obstacles are shown in **figure 1**.



Figure 1: Obstacles during the IGVC Competition

An example of what the obstacle course look like is shown in the **figure 2**.

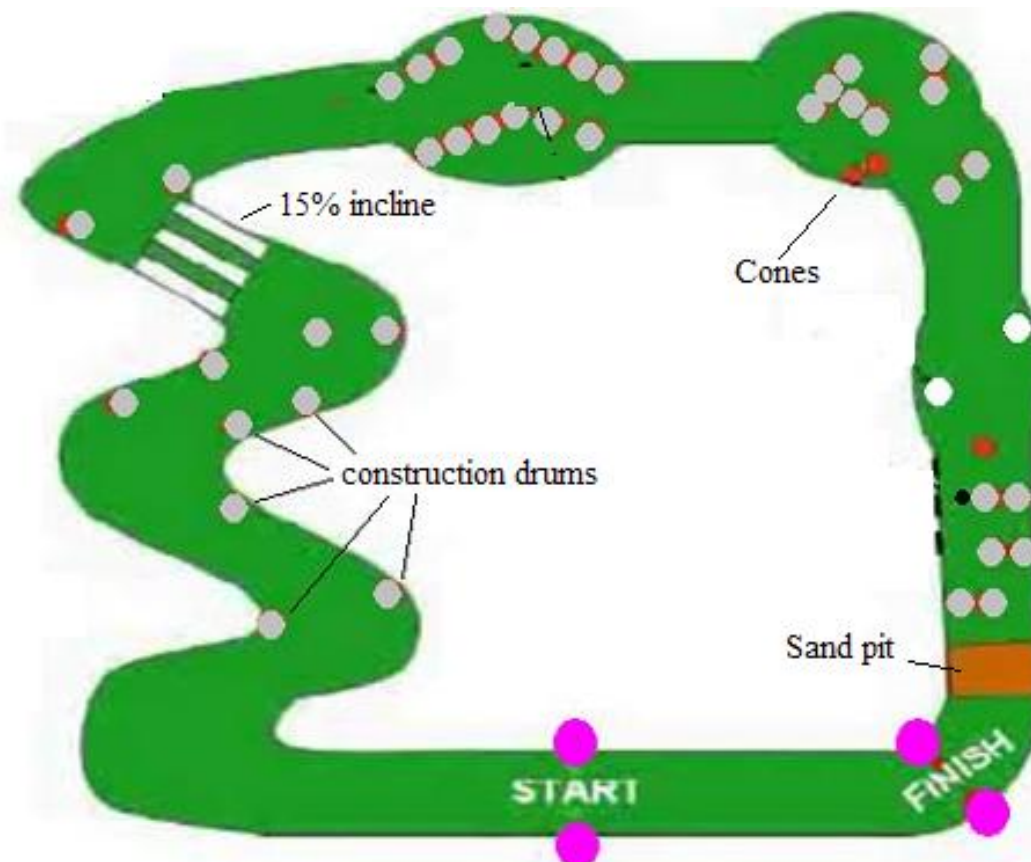


Figure 2: Top View of IGVC Obstacle Course

The survey of the competition site not only gave us better insight of the overview of the overall obstacle course, we also found a couple of common problem of the vehicles during the competition. Most of the vehicles have very slow acceleration. Whenever the vehicle making a turn or approaching obstacles, it would slow down considerably to avoid bumping into the obstacle or moving off the course. After it clears the obstacle, the vehicle will then slowly accelerates to find that it had to slow down again because of another obstacle. Because of the slow acceleration, most vehicles took a lot of time to finish certain distant. Since timing is one of the factors in winning the competition, our vehicle must be design for fast acceleration. Besides a high torque driving motors for fast acceleration, the overall mass of the vehicle has to be light.

Another common problem that we found during the competition was the poor maneuverability of the vehicles. Poor maneuverability contributed to the waste of time where redundant action had to be performed to overcoming obstacle. **Figure 3 and 4** shows one of the “dead spot” for the obstacle course during the competition. That was the place where most vehicles were disqualified from the competition by either bumping into the construction drum or making a wrong turn. The vehicle that managed to pass the obstacle wasted a lot of time because of the poor maneuverability.



Figure 3: A “dead spot” where vehicle slows down or fail the course



Figure 4: Closer view of the “dead spot”

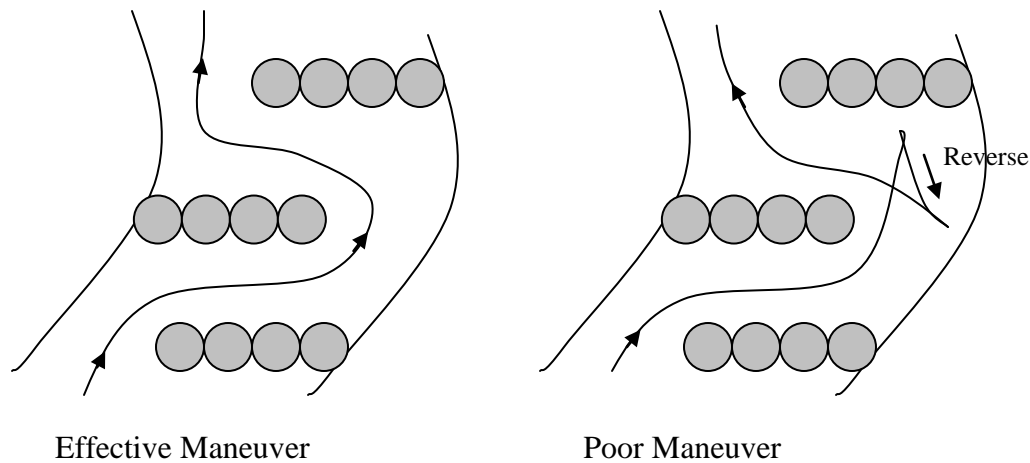


Figure 5: Maneuvering over a “dead spot” during the competition

Figure 5 shows the top view of the “dead spot”. A vehicle with an effective steering mechanism would have made a move as seen on the left. However, most vehicles during the competition had to make a three point turn as shown on the right of **figure 5** because of poor maneuverability. As can be seen, to make a zero point turn, the vehicle had to make a reverse move. Besides slowing down the vehicle, this move also compromises the effectiveness of obstacle detection of the vehicle. Since the front part of the vehicle has most obstacle detection devices (Sick Lidar, SONAR, camera), we would always want the orientation of vehicle to be facing front. To enable the vehicle to be able to safely make a reverse drive, we would need another set of expensive obstacle sensors on the back of the vehicle. The objective of the steering design is to effectively minimize the placement of the obstacle sensors on the back of the vehicle; where the steering pod enables all wheels drive and zero point turn to effectively maneuver through difficult obstacles and eliminate the need to make a reverse turn.

2.1 Objectives and Needs

After go through the rules of the competition, personally surveyed the competition ground and consideration for future upgrade, we came out with the objectives and needs for the design of steering system to ensure victory during competition. The needs are:

- a) Fast acceleration
- b) High maneuverability
- c) Modularity

For fast acceleration, we need high torque driving motor. In the design of steering pod, a lower mass will also give a higher acceleration. In this aspect, we utilized COSMOS for stress analysis and mass optimization.

The modularity aspect is to provide a design such that future team can easily upgrade the current system utilized.

For high maneuverability, the vehicle needs to be able to turn in the configurations shown in **figure 6**. For going straight, each wheel has to be parallel to the vehicle. For turning left, the front and back wheels need to point about North West. For turning right, the front and back wheels need to point about North East. The exact angle of the wheels depends on the turning radius of the vehicle. For zero point turn, each wheel has to turn 45 degree such that the radius of turning is right at the center of the vehicle.

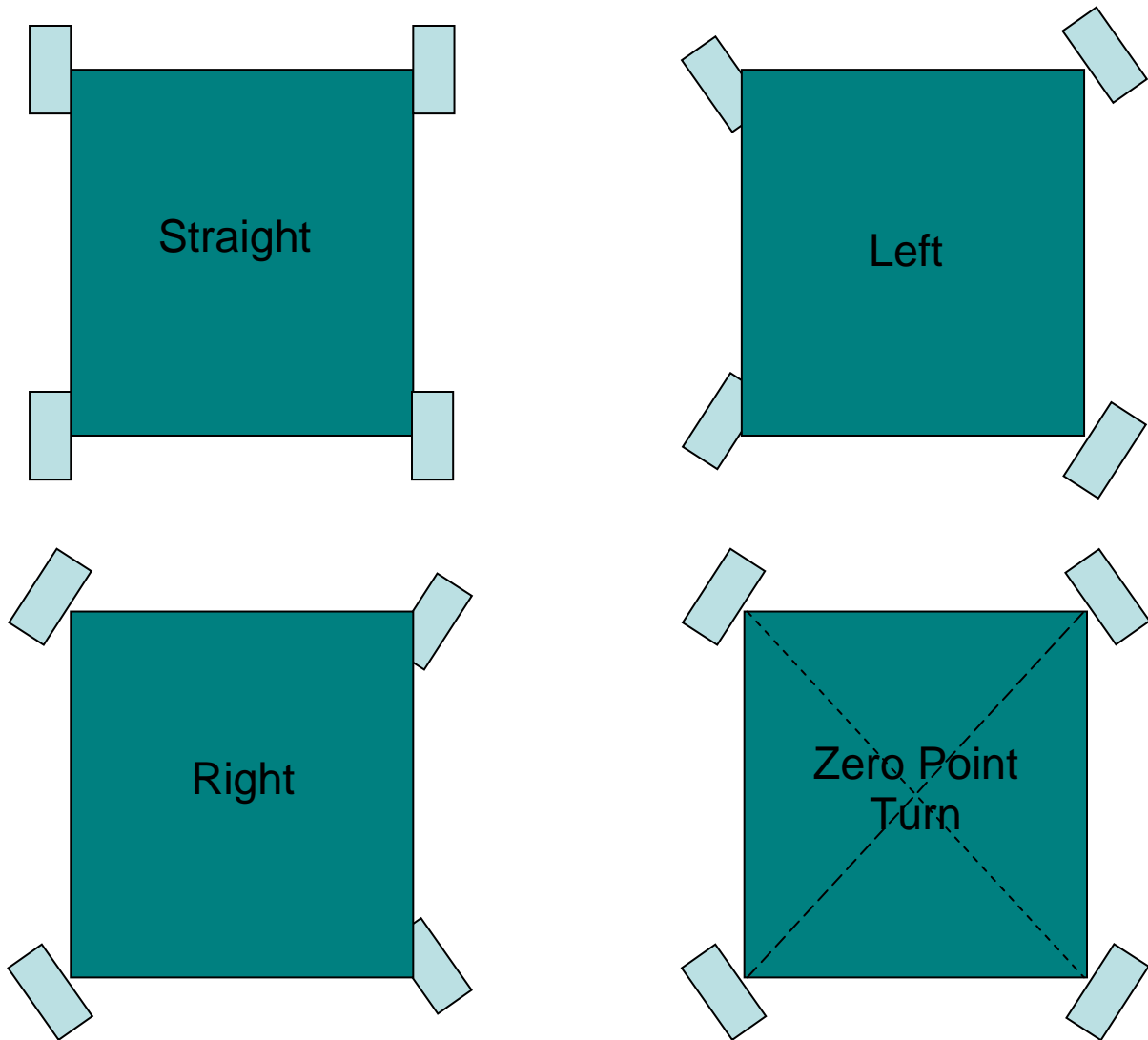


Figure 6: Configurations for different turnings

Having analyzed the different turning configurations, we observed a very important element for our design. In each different turnings (left, right, zero-point-turn), the top and bottom of the wheels will turn in different direction with same magnitude. For example, if the vehicle is steering left, we see that the top wheels rotates counter clockwise and the bottom wheels rotates clockwise with the same magnitude. We can essentially designing an actuator system to produce such wheels turning directions for effective maneuvering.

2.2 Design Choices

We came out with a few designs for steering mechanism. The designs are:

- a) Linkage bar steering
- b) Rotating shaft steering
- c) Gears, pulleys and belts steering

Linkage Bar Steering

The linkage bar steering design utilized two bars linking the motor bars and the wheel's bars. When the motor turns, the bar that is linked diagonally to the top wheel will produce the opposing turning direction of the motor to the wheel. The bar that is link straight down to the bottom wheel will produce same turning direction of the motor to the wheel. A clearer representation of the linkage bar design is shown in **figure 7**.

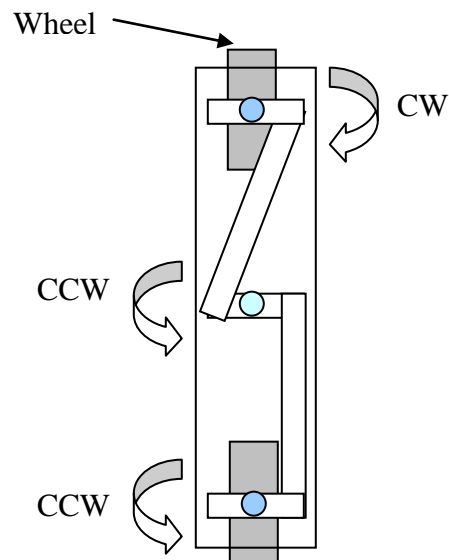


Figure 7: Linkage Bar Steering Mechanism

This idea seems functional at first glance. However, after further evaluation, we found out that this linkage bar steering system has a fundamental flaw in it. Although this design will generate opposite turning direction of the wheels, the magnitude of angle produced is different for top and bottom wheel. (Note that we need the top and bottom wheel to produce opposing turning direction with the same magnitude for effective steering) This problem is due to the fact that one bar is linked diagonally while one bar is linked straight, where upon turning by the motor, both of this linkages traveled different distances which produce different turning angle for top and bottom wheels. Because of this flaw, the design was discarded.

Rotating Shaft Steering

The rotating shaft design utilized worm gears and rotating shaft to make the opposing turning direction of the wheels. The steering motor will rotate the shaft in certain direction, the gearbox at the end of each wheels will then transfer the rotating shaft into the desired wheel turning direction. **Figure 8** shows the better representation of the rotating shaft steering design.

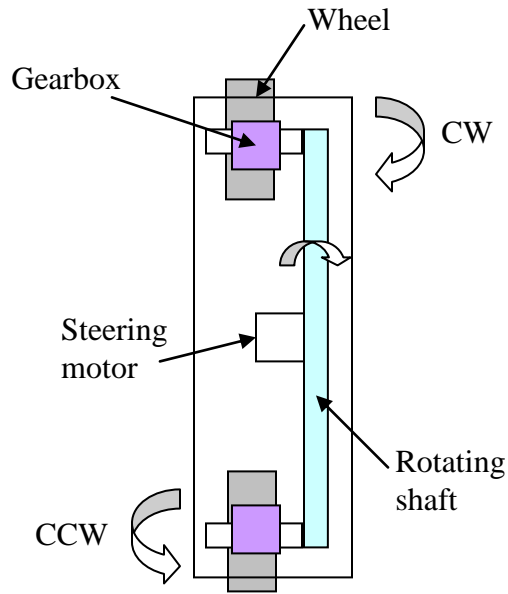


Figure 8: Rotating Shaft Steering Mechanism

The advantages of using this design is such that the worm gear prevents any back clash from the wheel. The wheel will only turn in the direction as instructed by the motor. However, the gearbox with the right specification is hard to find on the market and is very expensive.

Gears, Pulleys and Belts Steering

This design utilized gears, pulleys and belts to control the direction of the wheels. The gears serve to create an opposing motion and the pulleys and belts will transmit the opposing torque to the wheels. A clearer representation of the design is shown in **figure 9**.

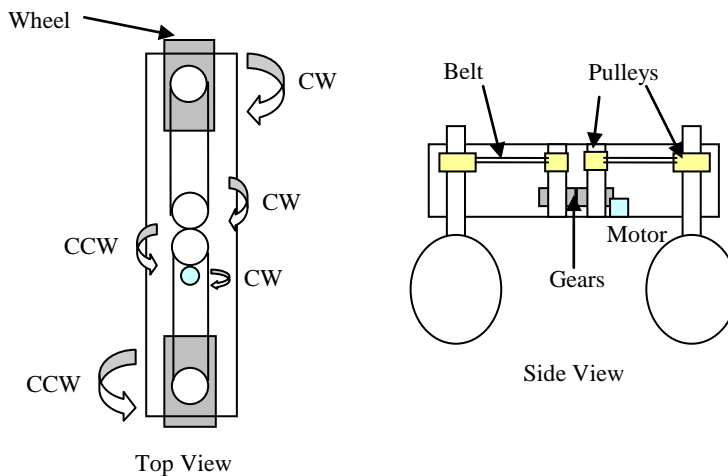


Figure 9: Gears, Pulleys and Belts Steering Mechanism

This design utilized components that are readily available. We can choose desired gears, pulleys and belts to obtain desired gear reduction and torque. The parts are also fairly cheap compared to other design. Because of the advantages of this design, we choose this design for the steering system.

3 DETAILED DISCUSSIONS

As mentioned in the previous section, gears, pulleys and belts are used for the steering system. The final CAD model of the steering pod is shown in **figure 10**.



Figure 10: "Steering Pod" Design

For better view of the internal section of steering pod, an exploded view of steering pod is shown in figure 11 with important components labeled.

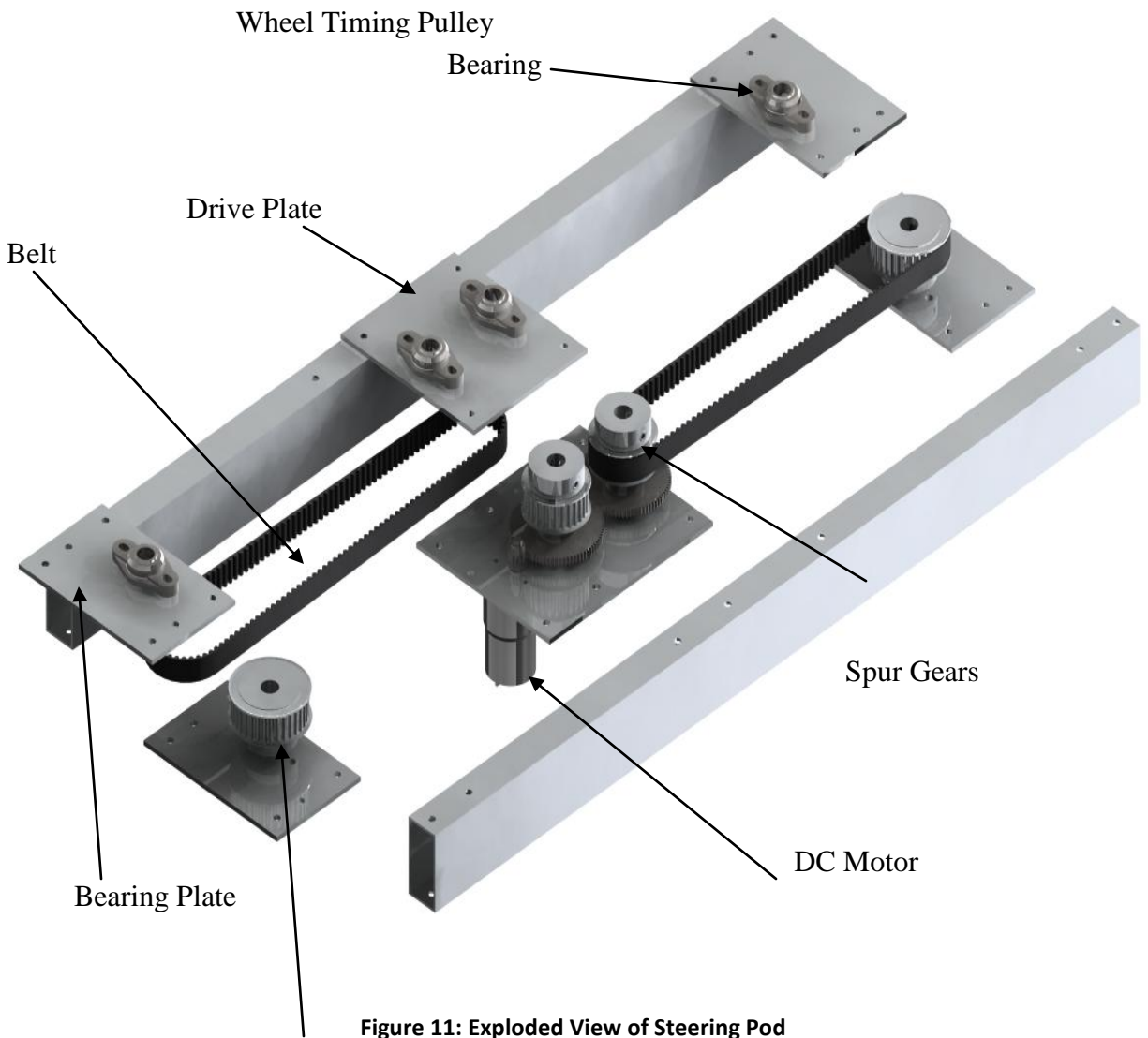


Figure 11: Exploded View of Steering Pod

The motor is connected to the two spur gears. The motor serves to provide torque for steering. The two spur gears serve to create two opposing torques. Connected to spur gear by shaft, the drive timing pulley will then transmit the torque to the timing belt which will then transmit to the wheel timing pulley. Using this method, we are able to produce same torque with different direction at both ends of the steering pod.

3.1 Calculation of Steering Torque

To determine which spur gears and pulleys to use with our steering motor, a steering torque T_s needed to be calculated. **Equation 3.1** can be used to calculate the steering torque.

$$\Sigma T = I * \alpha = T_s - T_f$$

$$T_s = I * \alpha + T_f \quad \text{-- 3.1}$$

where I is the drivetrain assembly moment of inertia, α is the angular acceleration, and T_f is the torque resulting from the friction between the tire and the ground.

Moment of Inertia about the steering shaft was determined by a complete drivetrain CAD model, with part densities, in SolidWorks and using its *mass properties calculator*. The CAD model of the drivetrain is shown in **figure 12**.

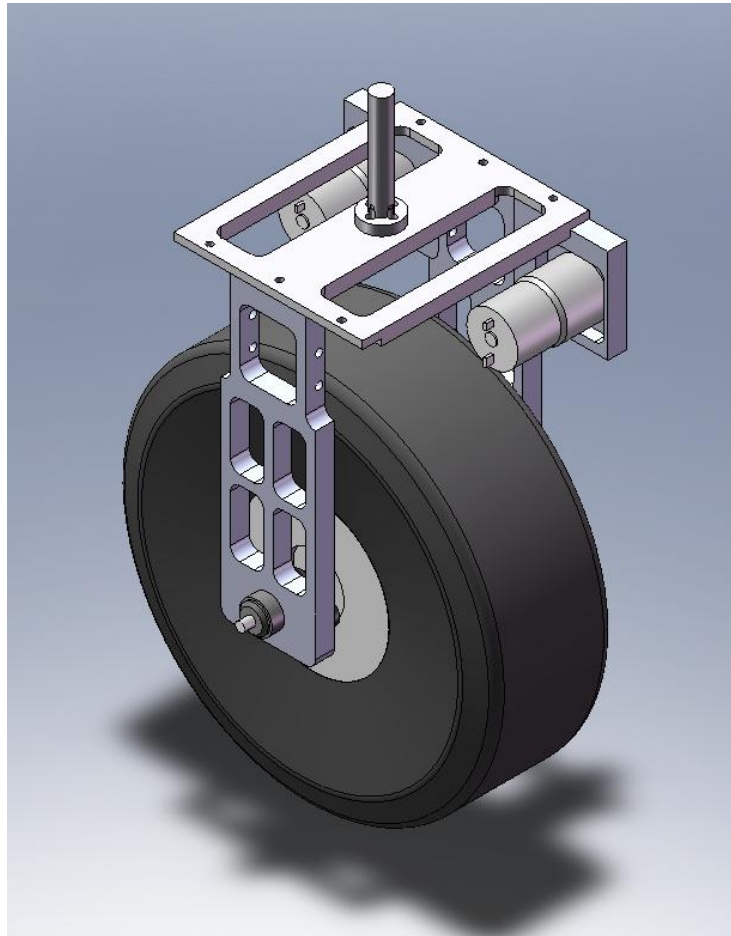


Figure 12: Drivetrain Design

From SolidWorks, the resulting moment of inertia is:

$$0.0104 \text{ kg/m}^3 + 0.0028 \text{ kg/m}^3 + 0.0002 \text{ kg/m}^3 = 0.0134 \text{ kg/m}^3$$

The desired angular turning displacement for the wheels is defined to be 90 degrees in one second. From this definition, the angular acceleration can be obtained from **equation 3.2**.

$$\theta = \frac{1}{2} \alpha * t^2$$

$$\alpha = \frac{2\theta}{t^2}$$

-- 3.2

The corresponding angular acceleration is 3.14 rad/s^2 .

Despite the complexity of ground-tire interactions, the analysis has to be done for accurate result. We decided to estimate the torque resulting from friction when steering using finite element analysis as shown below.

Viewing from the top, essentially, an $L \times W$ tire contact patch is defined and the resulting torque from infinitesimal patches is integrated to get the total steering torque as shown in **figure 13**.

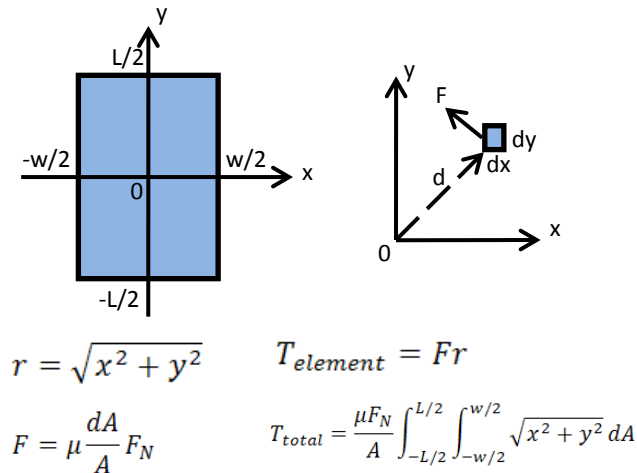


Figure 13: Integrating Contact Patch to Get Frictional Steering Torque

Since the integral cannot be solved by hand, Matlab is utilized to perform the double integral. Assuming

$L = 2.0$ in (Length of tire in contact with ground)

$W = 2.5$ in (Width of tire in contact with ground)

$\mu = 0.35$ (rubber-grass)

$F_N = 73.5$ N (Weight of vehicle)

The frictional steering torque is calculated to be 2.125 Nm. **Figure 14** shows how the T_f converges in Matlab plot. (See Appendix A for the Matlab code)

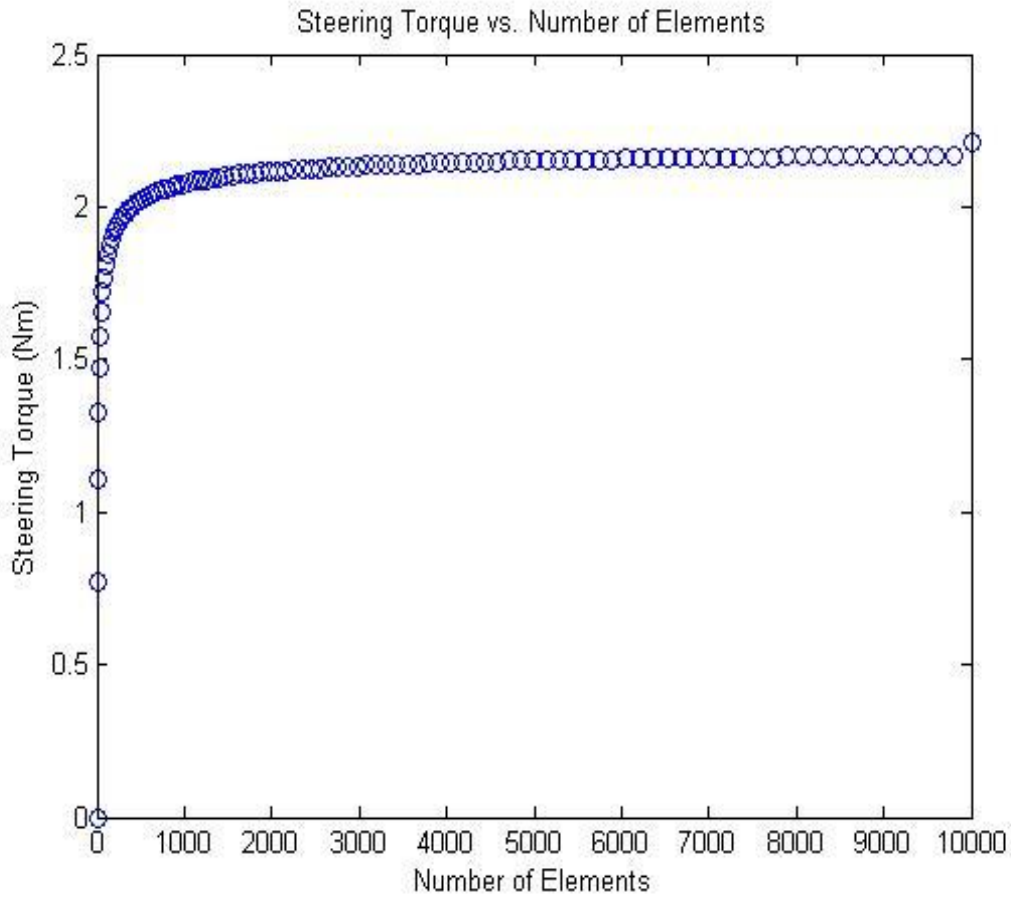


Figure 14: Frictional Steering Torque Convergence Plot

Knowing T_f , I , and α , we can then calculate the required steering torque per wheel, T_s from **equation 3.1**. T_s was then calculated to be 2.2238 Nm. It is observed that the main resistance to the steering results from the ground friction because of the small moment of inertia of the wheel assembly. With T_s , we can then select the appropriate gears, pulleys and belts for our steering system.

3.2 Gear Reduction Calculations

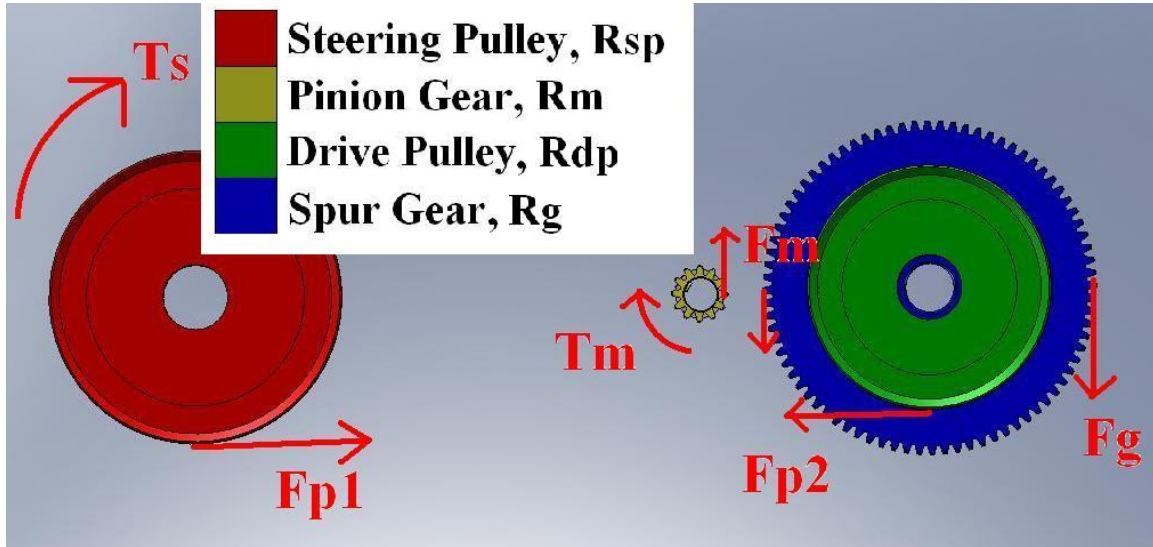


Figure 15: Free Body Diagram of Gears and Pulleys

The mechanical advantage between the steering torque T_s and the motor torque T_m was analytically found from the summation of torque about the drive pulley/spur gear shaft. Assuming the corresponding radii in **figure 15**, that moment of inertia, I for the spur gear/ drive pulley shaft is negligible, and that all forces are approximately tangential to their respective gears and pulleys, the torque about the drive pulley/ spur gear shaft can be written as:

$$\sum T = I * \alpha \cong 0 = (F_m - F_g) * R_g - F_{p2} * R_{dp} \quad \text{-- 3.3}$$

yielding a relation between the tangential motor and steering forces on the appropriate gears and pulleys. We know a simple relation that torque is equal to normal force times distance.

$$T_m = F_m * R_m \quad (\text{motor torque}) \quad \text{-- 3.4}$$

$$T_s = F_{p1} * R_{sp} \quad (\text{steering torque}) \quad \text{-- 3.5}$$

We also know that the torque produced by the force F_{p2} and F_g should be the same because both of them are lying on the same shaft.

$$\begin{aligned} F_{p2} * R_{dp} &= F_g * R_g \\ \Rightarrow F_{p2} &= F_g * R_g / R_{dp} \end{aligned} \quad \text{-- 3.6}$$

F_{p1} should be the same as F_{p2} as the belt serves to transmit the force. Using this relation, we get from **equation 3.6** that:

$$\begin{aligned} F_{p1} &= F_g * R_g / R_{dp} \\ \Rightarrow F_g &= F_{p1} * R_{dp} / R_g \\ \Rightarrow F_g &= T_s / R_{sp} * R_{dp} / R_g \end{aligned} \quad \text{-- 3.7}$$

Substituting **equation 3.4, 3.5, 3.7** in to **equation 3.3**, we get:

$$T_s = \frac{1}{2} * T_m * (R_g / R_m) * (R_{sp} / R_{dp}) \quad \text{-- 3.8}$$

If we were to interpret equation 3.8 literally, the torque produced by the motor is halved (because of distributing to both sides of wheels) and the gears and pulleys serve to increase the torque for steering.

Knowing that the torque needed for steering is 2.22N according to our specification, we choose a gears and pulleys such that if will produce enough torque to steer the wheels. We know that the motor will produce torque of 1.4 Nm. Choosing:

Spur Gear (Pitch: 32, Teeth: 12, H.D. 0.3750")

Spur Gear (Pitch: 32, Teeth: 80, H.D. 1.125")

Timing Pulley (GT2 5mm, 28 Grooves, P.D. 1.754")

Timing Pulley (GT2 5mm, 34 Grooves, P.D. 2.130")

We get steering torque of 2.55Nm, which is enough for steering. We can increase the pressure of the wheels to decrease the contact patch on the ground (to reduce the frictional steering torque) for better steering.

3.3 Stress Analysis on Various Components

Stress analysis was done on various components to optimize the mass and to make sure that the component will not fail.

Bearing Plate Analysis

The $\frac{1}{4}$ " thick plates used in the first prototype were contributing significantly to the weight of the assembly. In an attempt to reduce mass, the possibility of reducing the plate thickness was examined. It was found that $\frac{1}{8}$ " plates would still support the load, while literally halving the mass of the part. **Figure 16** shows the boundary conditions for the bearing plate.

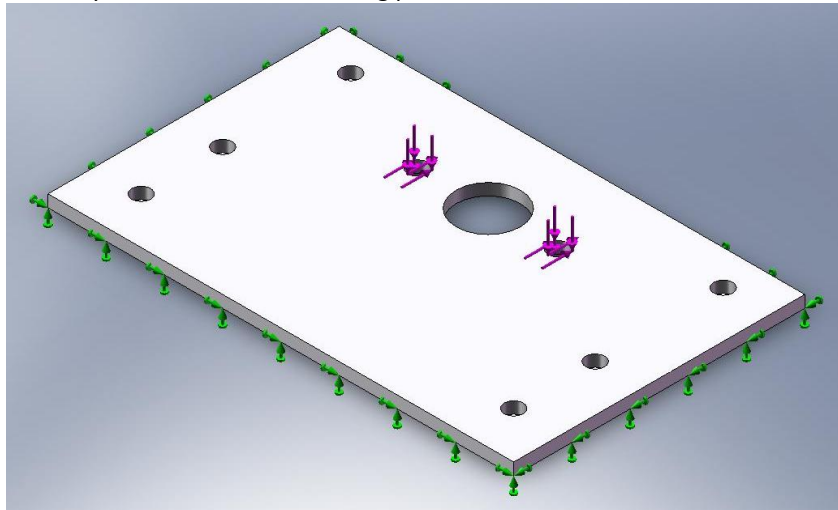


Figure 16: Boundary Conditions For Bearing Plate

The areas of the plate contacting its supporting beams were taken as fixed surfaces. Then, a vertical load equal to $\frac{1}{4}$ the weight of the robot, and a horizontal load equal to $\frac{1}{4}$ the driving force, were added to the surfaces of the bearing mount holes. Several meshes were created and run until convergence was attained. **Figure 17** shows the stress distribution on the bearing plate.

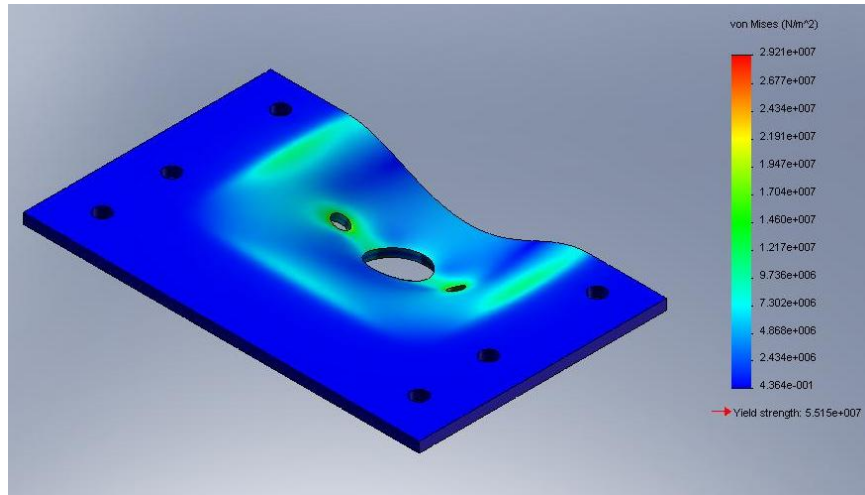


Figure 17: Stress Distribution on the Bearing Plate

With the von Mises stress plotted, the factor of safety on the plate is found to be 4.48 as shown in table below.

Study	Nodes	Elements	Stress (MPa)	% Difference
1	15830	8395	18.99	-
2	36755	21470	29.5	35.63%
3	95909	58669	29.21	0.99%

Yield Stress: 131
Actual Stress: 29.21

Factor of Safety: 4.48

Cross Beam Analysis

The cross beam is the two structural components connecting the two steering pod. For stress analysis, assuming that the beam is fixed at both end and the payload weight of 147N is distributed over the cross bar, we are able to perform structural analysis on the beam.

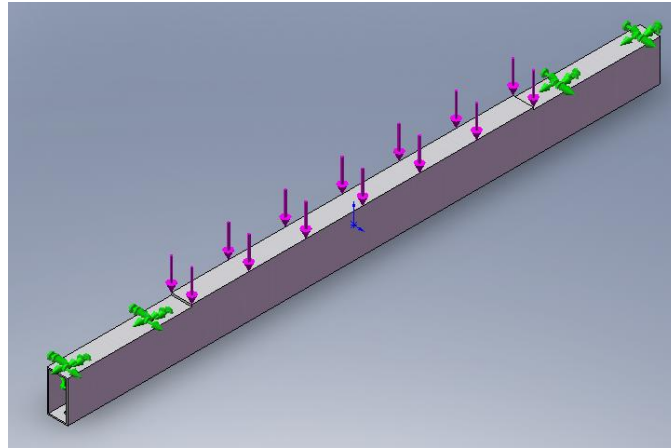
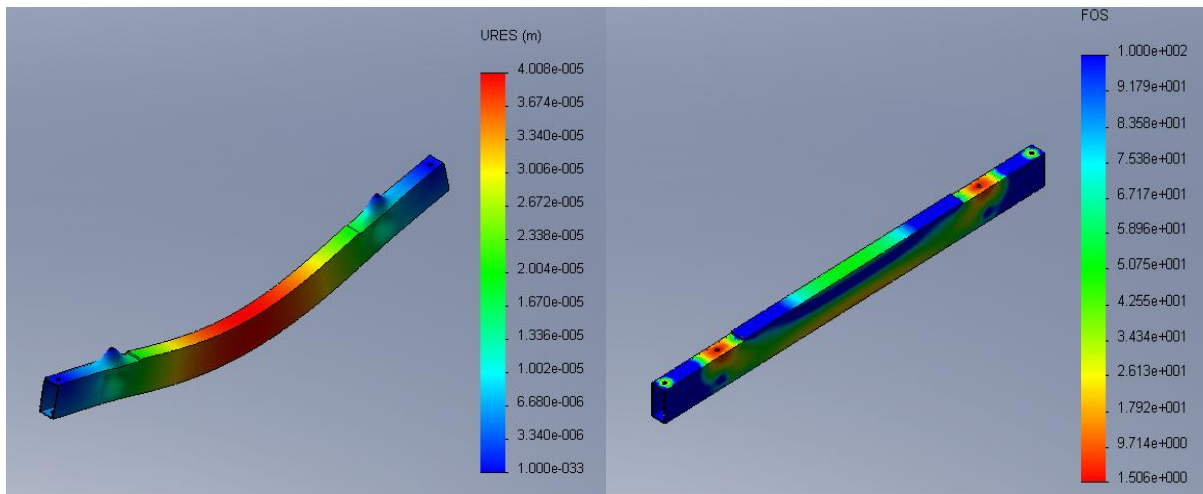


Figure 18: Boundary Conditions for Cross Beam



Spur Gear Analysis

Spur gears are used to create opposing torque with same magnitude. The inner cylindrical surface of the gear is fixed and a conservative force of 70 N (torque of about 2Nm) is applied to one of the tooth of the gear (Only one tooth of the gear is in contact with the other gear). **Figure 20 and 21** shows the displacement and factor of safety of the gear.

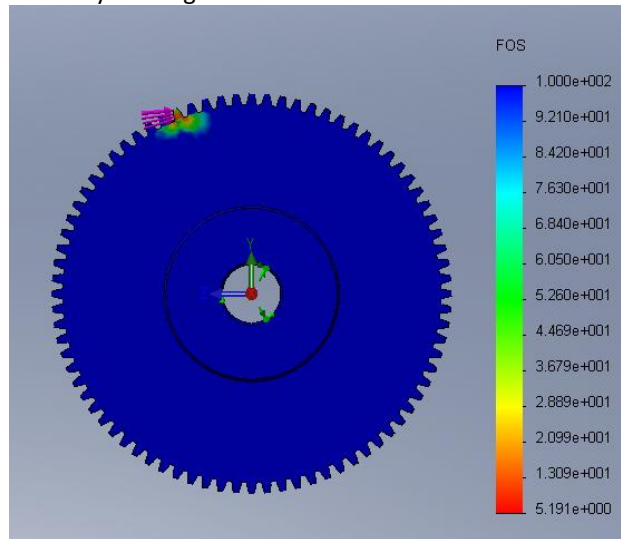


Figure 20: Factor of Safety of the Spur Gear

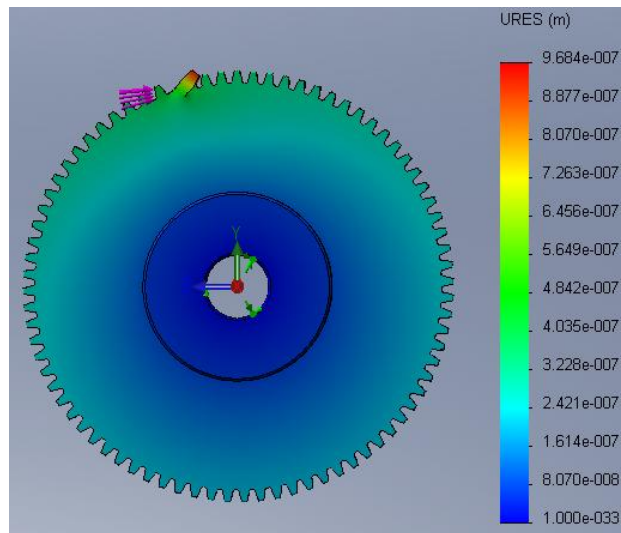


Figure 21: Displacement of the Spur Gear

As can be seen, we have factor of safety of more than 5. We also can safely assume that the gears will not get stuck because of deformation from the low displacement.

Timing Pulleys Analysis

The Timing Pulleys is made of 7074 Aluminum Alloy with yield strength of 400MPa. Using conservative assumption of 3 Nm of torque applied to the pulleys, the force exerted on the pulleys are 53.2N. We also know that there are 17 grooves in contact with the belt from the manufacture website. Therefore, dividing 53.2N by 17, we get force of 3.13N exerted on each groove of the pulleys. Using this information, we can then set the boundary conditions for analysis. **Figure 22** shows that the maximum stress occurs at the inner pulley. We have factor of safety over thousands. **Figure 23** shows the deformation plot of the material. The deformation is also negligible.

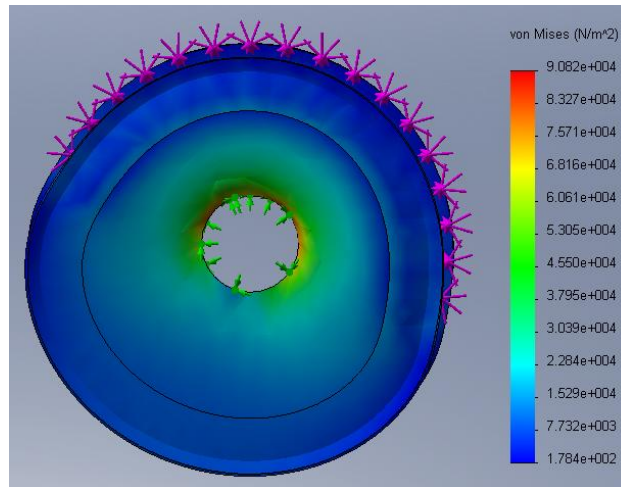


Figure 22: Pulley's Stress Distribution Plot

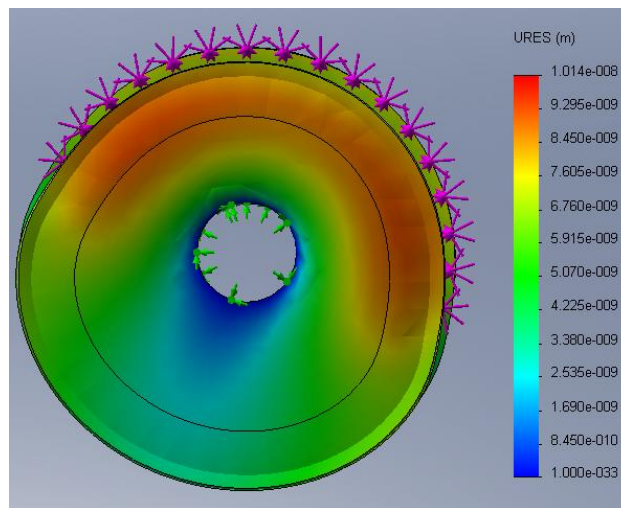


Figure 23: Pulley's Deformation Plot

3.4 Encoder

Encoder is used to determine the turning angle of the wheels. For our steering system, absolute shaft position is crucial which is why an absolute encoder is needed. With cost and functionality in mind, the Absolute Magnetic Encoder MAE3 from US Digital was chosen. For easy control, an analog output encoder is used where the output voltage is linearly proportional to the angle. **Figure 24** shows the plot of output voltage versus position given by the encoder.

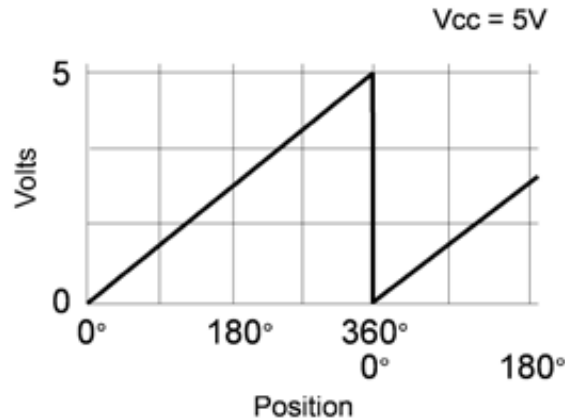


Figure 24: Encoder Output Voltage vs. Position

3.5 Prototyping

With the analysis of various components, the design phase of steering pos was completed. We then ordered the beams, plates, gears, pulleys and belts according to the calculated dimensions. When the stocks arrived, we hurriedly machine one side of the steering pod so that we have a concrete model to analyze. After a week of fabrication, the first prototype was done and assembled. The steering pod weighs about 3.8kg. With first prototype, it was proven that the steering design is workable. A new set of steering pod is currently being fabricated, with some adjustment to weight and length of the steering pod. Refer to APPENDIX B for the drawings of all the parts.

4 CONCLUSIONS

This steering system serves its objective well where it will provide an effective steering mechanism for the team during IGVC competition. The steering system enables the vehicle to steer left, right and make a zero point turn.

Steering Specifications

- Angular Acceleration: 3.14 rad/s^2
- Gear and Pulley reduction: ~ 4
- Torque per motor: 1.4 Nm
- Maximum Torque: 2.5 Nm
- Weight: $\sim 3.5 \text{ kg}$

Parts List and Cost

Table below shows the parts list and cost for the whole steering system.

Part	Part #	Supplier	Price	Quantity	Total
1" x 2" x 1/16" Aluminum Rectangle Tube (36" Length)	-	OnlineMetals	\$9.18	8	\$73.44
1/8" x 5" Aluminum Flat Bar (48" Length)	F4185	MetalsDepot	\$19.40	2	\$38.80
Spur Gear (Pitch: 32, Teeth: 12, D.P. 0.3750")	S1084Z-032S012	SDP-SI	\$10.99	2	\$21.98
Spur Gear (Pitch: 32, Teeth: 80, D.P. 0.3750")	A 1C 2-N32080	SDP-SI	\$22.00	4	\$88.00
Timing Pulley (GT2 5mm, 28 Grooves)	A 6A55-028DF1516	SDP-SI	\$14.87	4	\$59.48
Timing Pulley (GT2 5mm, 34 Grooves)	A 6A55-034DF1516	SDP-SI	\$16.44	4	\$65.76

Timing Belt (GT2 5mm)	A 6R55M140150	SDP-SI	\$19. 65	2	\$39.3 0
#10-32 Nut, 1/8" Height	90480A195	McMaster	\$1.3 8	1	\$1.38
#10 Washer, 1/2" Diameter, 0.052" Height	91090A103	McMaster	\$3.8 8	1	\$3.88
#10 Split Washer, 3/64" Thickness	91102A740	McMaster	\$0.9 5	1	\$0.95
#10 Threaded Rod, 3" Length	95475A513	McMaster	\$7.8 7	2	\$15.7 4
#10 Socket Head Cap Screw, 5/8" Length	91251A344	McMaster	\$10. 64	1	\$10.6 4

TOTAL:	\$419.35
---------------	-----------------

Future Plan

By the end of this semester, the main chassis will be done as shown in figure 25. Mass optimization and improvement of the current design will also be considered for best steering performance.

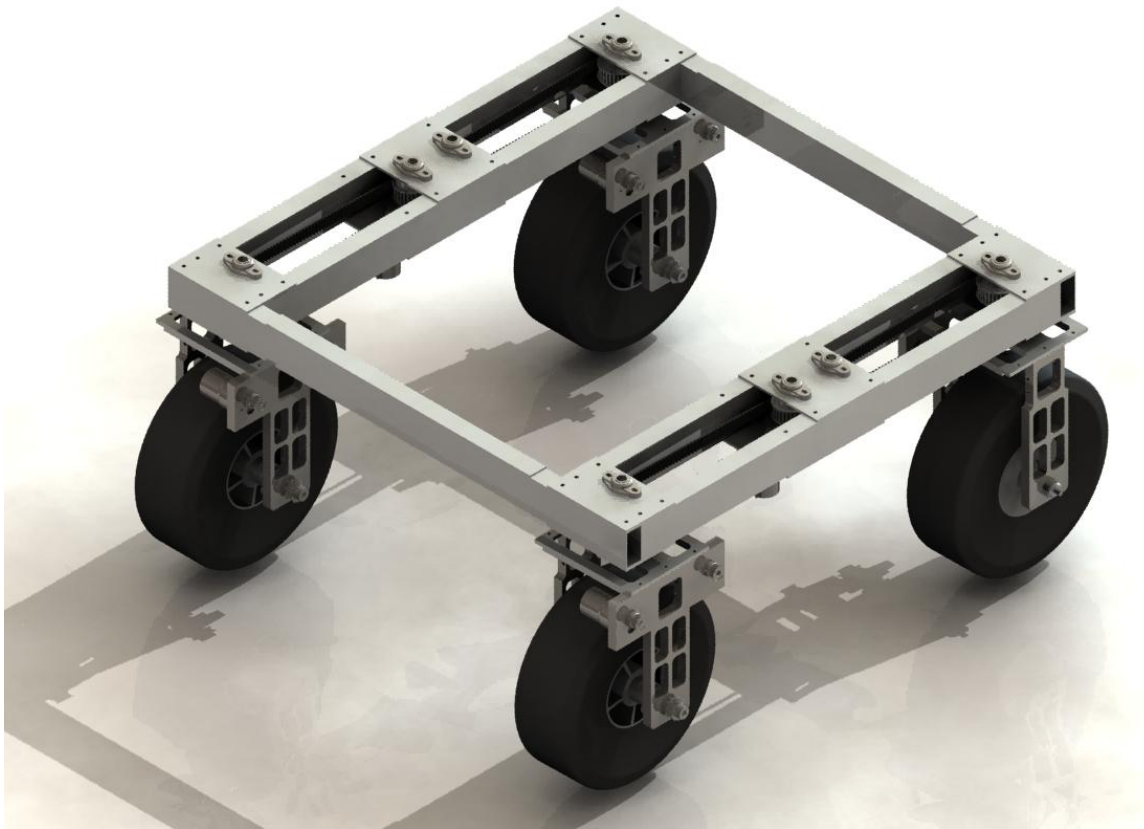


Figure 25: Chassis of Gladiator

The payload frame is currently under development and the Gladiator should look as shown in **figure 26**.

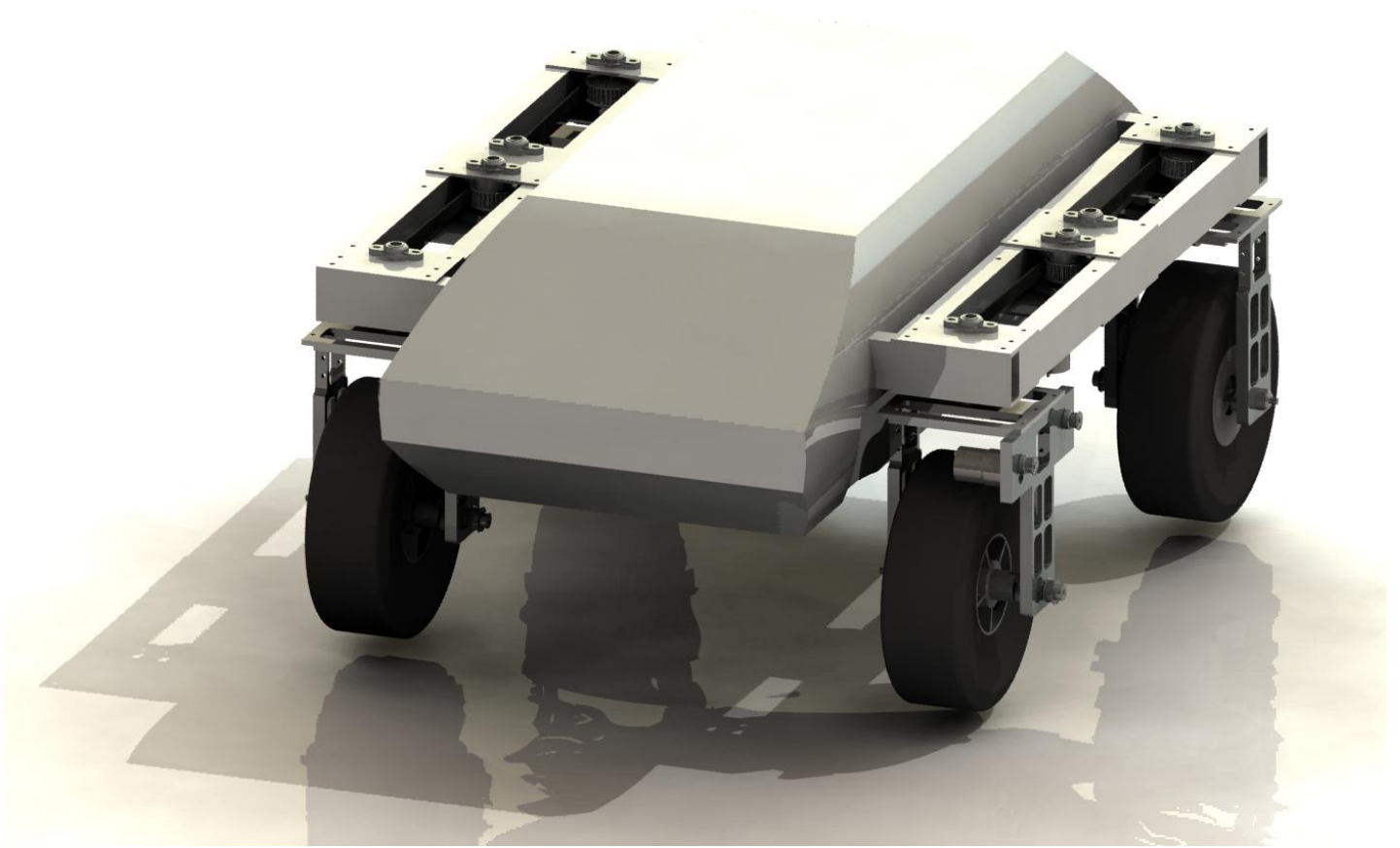


Figure 26: Gladiator

APPENDIX A

Matlab code for frictional torque calculation

```
function plottorques
```

```
clc;
```

```
close all;
```

```
divs = linspace(0, 100);
```

```
for i = 2 : length(divs)
```

```
plot(divs(i) ^ 2, steeringtorque(divs(i)), 'bo');
```

```
hold on;
```

```
end
```

```
ylabel('Steering Torque (Nm)');
```

```
xlabel('Number of Elements');
```

```
title('Steering Torque vs. Number of Elements');
```

```
end
```

```
function torque = steeringtorque(divs)
```

```
%finds steering torque component from upper right quadrant of
```

```
%contact area and multiplies by 4 to get nominal torque
```

```
%divs = 50; %divisions per quadrant
```

```
mu = 0.35;
```

```
safety = 1;
```

```
xcorner = 1.25 * 0.0254; %inches
```

```
ycorner = 1 * 0.0254; %inches
```

```
X = linspace(0, xcorner, divs); %X vector
```

```
Y = linspace(0, ycorner, divs); %Y vector
```

```
R = zeros(length(X) - 1, length(Y) - 1);
```

```
delx = xcorner/divs / 2;
```

```
dely = ycorner/divs / 2;
```

```
forceperpt = 30 * 9.8 / 4 / divs^2;
```

```
if delx > 0.00001 && dely > 0.00001
```

```
for i = 2 : length(X)
```

```
for j = 2 : length(Y)
```

```
R(i,j) = ((X(i)-delx)^2 + (Y(j)-dely)^2)^.5;
```

```
end
```

```
end
```

```
torque = 4 * sum(sum(R)) * mu * safety * forceperpt;
```

```
%msgbox(['Steering torque is ' num2str(torque) 'lb-in' ]);
```

```
else
```

```
torque = 0;
```

```
end
```

```
end
```

APPENDIX B

